



Article

# Essential Oils from Mediterranean Plants Inhibit In Vitro Monocyte Adhesion to Endothelial Cells from Umbilical Cords of Females with Gestational Diabetes Mellitus

Valeria Schiavone <sup>1,2,†</sup>, Tea Romasco <sup>1,2,†</sup>, Nadia Di Pietrantonio <sup>1,2</sup>, Stefania Garzoli <sup>3</sup>, Carola Palmerini <sup>1,2</sup>, Pamela Di Tomo <sup>1,2</sup>, Caterina Pipino <sup>1,2</sup>, Domitilla Mandatori <sup>1,2</sup>, Rossella Fioravanti <sup>3</sup>, Elena Butturini <sup>4</sup>, Manuela Sabatino <sup>5</sup>, Maria Pompea Antonia Baldassarre <sup>2,6</sup>, Rino Ragno <sup>5,\*</sup>, Assunta Pandolfi <sup>1,2</sup> and Natalia Di Pietro <sup>1,2,\*</sup>

- <sup>1</sup> Department of Medical, Oral and Biotechnological Sciences, “G. d’Annunzio” University of Chieti-Pescara, 66100 Chieti, Italy
  - <sup>2</sup> Center for Advanced Studies and Technology—CAST, “G. d’Annunzio” University of Chieti-Pescara, 66100 Chieti, Italy
  - <sup>3</sup> Department of Pharmaceutical Chemistry and Technology, Sapienza University of Rome, 00185 Roma, Italy
  - <sup>4</sup> Department of Neurosciences, Biomedicine and Movement Sciences, Section of Biochemistry, University of Verona, 37129 Verona, Italy
  - <sup>5</sup> Rome Center for Molecular Design-RCMD, Department of Pharmaceutical Chemistry and Technology, Sapienza University of Rome, 00185 Roma, Italy
  - <sup>6</sup> Department of Medicine and Aging Sciences, “G. d’Annunzio” University Chieti-Pescara, 66100 Chieti, Italy
- \* Correspondence: rino.ragno@uniroma1.it (R.R.); natalia.dipietro@unich.it (N.D.P.)
- † These authors equally contributed to this work.



**Citation:** Schiavone, V.; Romasco, T.; Di Pietrantonio, N.; Garzoli, S.; Palmerini, C.; Di Tomo, P.; Pipino, C.; Mandatori, D.; Fioravanti, R.; Butturini, E.; et al. Essential Oils from Mediterranean Plants Inhibit In Vitro Monocyte Adhesion to Endothelial Cells from Umbilical Cords of Females with Gestational Diabetes Mellitus. *Int. J. Mol. Sci.* **2023**, *24*, 7225. <https://doi.org/10.3390/ijms24087225>

Academic Editor: William N. Setzer

Received: 16 January 2023

Revised: 11 April 2023

Accepted: 12 April 2023

Published: 13 April 2023



**Copyright:** © 2023 by the authors. Licensee MDPI, Basel, Switzerland. This article is an open access article distributed under the terms and conditions of the Creative Commons Attribution (CC BY) license (<https://creativecommons.org/licenses/by/4.0/>).

**Abstract:** Essential oils (EOs) are mixtures of volatile compounds belonging to several chemical classes derived from aromatic plants using different distillation techniques. Recent studies suggest that the consumption of Mediterranean plants, such as anise and laurel, contributes to improving the lipid and glycemic profile of patients with diabetes mellitus (DM). Hence, the aim of the present study was to investigate the potential anti-inflammatory effect of anise and laurel EOs (AEO and LEO) on endothelial cells isolated from the umbilical cord vein of females with gestational diabetes mellitus (GDM-HUVEC), which is a suitable in vitro model to reproduce the pro-inflammatory phenotype of a diabetic endothelium. For this purpose, the Gas Chromatographic/Mass Spectrometric (GC-MS) chemical profiles of AEO and LEO were first analyzed. Thus, GDM-HUVEC and related controls (C-HUVEC) were pre-treated for 24 h with AEO and LEO at 0.025% *v/v*, a concentration chosen among others (cell viability by MTT assay), and then stimulated with TNF- $\alpha$  (1 ng/mL). From the GC-MS analysis, trans-anethole (88.5%) and 1,8-cineole (53.9%) resulted as the major components of AEO and LEO, respectively. The results in C- and GDM-HUVEC showed that the treatment with both EOs significantly reduced: (i) the adhesion of the U937 monocyte to HUVEC; (ii) vascular adhesion molecule-1 (VCAM-1) protein and gene expression; (iii) Nuclear Factor-kappa B (NF- $\kappa$ B) p65 nuclear translocation. Taken together, these data suggest the anti-inflammatory efficacy of AEO and LEO in our in vitro model and lay the groundwork for further preclinical and clinical studies to study their potential use as supplements to mitigate vascular endothelial dysfunction associated with DM.

**Keywords:** essential oils; anise; laurel; anti-inflammatory; HUVEC; VCAM-1; inflammation; diabetes; NF- $\kappa$ B p65; endothelial dysfunction

## 1. Introduction

Essential oils (EOs) are heterogeneous mixtures of numerous volatile compounds produced by plants' secondary metabolism able to capture the plants' scent and flavor [1]. Monoterpenes, sesquiterpenes, and related oxygenated derivatives are the main components of EOs, which provide them with biological properties and the characteristic essence.

In addition to these, EOs also consist of a minor amount of aliphatic and aromatic compounds derived from phenylpropane, all characterized by a low molecular weight. It is important to underline that, as reported by the literature, the final chemical composition also depends on the extraction methods. In this regard, EOs can be obtained through distillation (via steam and/or water) or mechanical methods, such as cold pressing [2]. In any case, the bioactivities of a particular EO are mostly related to the synergistic effects of several chemical constituents, while no individual compounds show bioactivity [3].

Much evidence from in vitro and animal studies proves that EOs have multiple biological activities, such as anticancer [4,5], antiviral [6–9], antibacterial [10–13], antifungal [14,15], antibiofilm [16–18], anti-inflammatory [19–21], and antioxidant [19,22–25] effects, which constitute the starting point for the in vivo assessment of those properties in various therapeutic and cosmetic fields [26–33]. Nevertheless, since great consideration has been given to the effective use of EOs in clinical procedures, further systematic animal studies and clinical investigations are needed. In recent years there has been a growing interest in the study of EOs for their potential beneficial effects on diabetes mellitus (DM) and metabolic diseases related to obesity [3,34–36].

As a matter of fact, it has been observed that the possible use of EOs and some of their isolated constituents, such as monoterpenoids, improve and reduce the risk factors associated with cardiovascular diseases [37]. In particular, the study of Rajeshwari et al. [38] showed a significant reduction in fasting blood glucose levels following a daily treatment of 60 days with anise seeds powder in 20 patients with type 2 DM (in the age group of 40–60 years with no other specific complications). Interestingly, the antidiabetic, hypolipidemic, and antioxidant activities were a result of the synergistic action of antioxidants and phytochemicals (e.g.,  $\beta$ -carotene, Vitamin A, C, and E) present in the anise seeds. In addition, other animal studies suggested that anise extracts could play an important role in blood glucose and type 2 DM management [39].

Along with anise, a recent study [40] showed that the leaf extract of another typical Mediterranean plant, *Laurel nobilis*, significantly decreased blood glucose levels and restored altered liver enzymes, urea, creatine kinase, total protein levels, calcium, and ferritin in six streptozotocin (STZ)-induced DM rats after a daily consumption period of 28 days when compared to the same number of untreated diabetic rats. Alam Khan et al. [41] have also proved that the encapsulation of 1, 2, or 3 g of ground bay leaves significantly reduces serum glucose, total cholesterol, Low-Density Lipoprotein (LDL) cholesterol, and triglycerides, and increases the High-Density Lipoprotein (HDL) cholesterol levels after 30 days in patients with type 2 DM with respect to a placebo group (a total of 40 individuals with more than 40 years were included and continued their normal diets and diabetic medications, except for insulin therapy, throughout the study). In relation to this, the positive effects of anise and laurel consumption on reducing the risk of cardiovascular disease were demonstrated, significantly improving the lipid profile with the increase of HDL cholesterol concentration and the decrease of LDL, not only in patients with type 2 DM but also in healthy people [41,42]. More specifically, in several in vitro and animal studies, it could be found that the phenolic acids and flavonoids contained in anise, such as *p*-coumaric acid, gallic acid, cinnamic acid, chlorogenic acid, and ferulic, besides catechin and rutin, contributed to prominently affecting the HDL lipid composition and to its atheroprotective action, exhibiting a radical scavenging activity, together with 1,8-cineol and other components (eugenol, acetyl and methyl eugenol,  $\alpha$ - and  $\beta$ -pinene, phellandrene, linalool, geraniol, and terpineol) of laurel [43–45]. Unfortunately, nowadays most of the studies that can be found in the literature are based on cell culture or animal models rather than human studies, yet their effectiveness in humans is necessary to confirm through future research. Despite this, on this basis, it is possible to consider that both anise and laurel EOs (AEO and LEO, respectively) may serve as support for the management of type 2 DM and cardiovascular disease. However, to date, there is no evidence of their efficacy in improving or preventing endothelial dysfunction, which is considered one of the first steps in the atherosclerotic process associated with DM.

In this regard, in presence of persistent hyperglycemia, the activity of nitric oxide (NO) in preventing leukocyte adhesion and maintaining the endothelium in an anti-inflammatory state is compromised and the transcription factor Nuclear Factor-kappa B (NF- $\kappa$ B) p65 signaling pathway is activated [46–49]. In turn, this latter induces the expression of cytokines, chemokines, and adhesion molecules, such as Vascular Cell Adhesion Molecule-1 (VCAM-1), Intercellular Adhesion Molecule-1 (ICAM-1), and E-selectin, which participate in the recruitment of monocytes to the endothelial surface, playing a key role in the onset of inflammation and endothelial dysfunction, as well as in the progression of diabetic vascular complications [50,51].

The mechanisms determining the development of endothelial dysfunction are complex and not limited only to hyperglycemia. For example, during pregnancies complicated by diabetes and/or obesity, although also present in physiologically normal pregnancies, an increase of circulating inflammatory molecules and reduced levels of anti-inflammatory molecules, such as IL-10 and adiponectin, were demonstrated [52]. Gestational diabetes mellitus (GDM) later leads to an imbalance between pro- and anti-inflammatory/oxidative molecules that may support the development of early vascular senescence and endothelial dysfunction in offspring [53]. In general, the chronic state of low-grade inflammation caused by obesity is known to interfere with the normal transmission of insulin signaling, favoring the onset of type 2 DM and further propagating the state of chronic inflammation and vascular dysfunction even years before the diagnosis of diabetes [34,54]. Based on the above premises, the present study was undertaken to investigate the potential anti-inflammatory role of AEO and LEO on primary endothelial cell cultures isolated from the umbilical cord vein of females with gestational diabetes mellitus (GDM-HUVEC), which represent a valuable *in vitro* model for reproducing the *in vivo* pro-inflammatory vascular phenotype associated with chronic hyperglycemia [55]. In particular, the use of AEO and LEO is proposed to contribute to decrease the burden of inflammation in vascular cells by targeting the earlier altered mechanisms involved in the onset of endothelial dysfunction.

## 2. Results

### 2.1. Chemical Composition of EOs

The chemical characterization of AEO and LEO was performed by Gas Chromatographic/Mass Spectrometric (GC-MS) analysis. In total, 22 components were identified and listed in Table 1. The monoterpene content found in LEO (93.9%) is markedly higher than that found in AEO (3.8%), where *trans*-anethole (88.5%) was the most abundant component followed by estragole (3.8%) and *p*-anisaldehyde (2.1%). On the other side, 1,8-cineole (53.9%) and  $\alpha$ -terpinyl acetate (18.8%) were the molecules with higher percentage mean values detected in LEO.

### 2.2. Effects of AEO and LEO on Cell Viability

First, the potential cytotoxic effect of EOs derived from anise and laurel plants, both widely spread throughout the Mediterranean basin, was evaluated. For this purpose, the 3-(4,5-dimethylthiazolyl-2)-2, 5-diphenyltetrazolium bromide (MTT) cell viability assay was performed on GDM-HUVEC and related controls (C-HUVEC) treated with three different concentrations of AEO and LEO (0.025, 0.05, and 0.1% *v/v*) for 24 h and 48 h. The obtained results showed that C- and GDM-HUVEC viability remained stable and was not altered by treatment with AEO and LEO at all concentrations tested (Figure 1).

**Table 1.** AEO and LEO chemical composition.

N.	Component <sup>1</sup>	LRI <sup>2</sup>	LRI <sup>3</sup>	AEO% <sup>4</sup>	LEO% <sup>5</sup>
1	$\alpha$ -pinene	1018	1021	0.3	3.2
2	$\beta$ -pinene	1091	1099	-	2.3
3	sabinene	1110	1115	-	3.2
4	limonene	1198	1190	1.6	2.0
5	1,8-cineole	1201	1206	-	53.9
6	$\gamma$ -terpinene	1240	1244	-	1.8
7	o-cymene	1279	1287	-	2.4
8	linalool	1545	1547	0.9	3.0
9	$\alpha$ -bergamotene	1581	1582	0.5	-
10	terpinen-4-ol	1606	1603	0.3	3.0
11	$\beta$ -caryophyllene	1612	1619	0.4	-
12	estragole	1652	1655	3.8	-
13	$\alpha$ -terpinyl acetate	1685	1683	-	18.8
14	$\alpha$ -terpineol	1722	1719	0.2	-
15	myrtenol	1808	1804	-	0.3
16	trans-anethole	1840	1837	88.5	-
17	(E)-nerolidol	2025	2023	0.3	-
18	<i>p</i> -anisaldehyde	2030	2027	2.1	-
19	methyl eugenol	2036	2033	-	4.2
20	<i>p</i> -acetonylanisole	2172	2170	0.9	-
21	eugenol	2175	2172	-	1.9
22	isohomogenol	2191	2189	0.2	-
SUM				100.0	100.0
Monoterpenes				3.8	93.9
Sesquiterpenes				0.7	-
Other				95.5	6.1

<sup>1</sup> The components are reported according to their elution order on Stabilwax polar column; <sup>2</sup> linear retention indices (LRI) measured on a polar column; <sup>3</sup> LRI from the literature (Nist); <sup>4</sup> percentage mean values of AEO components (%); <sup>5</sup> percentage mean values of LEO components; \* LRI not available; - Not detected.

Moreover, the graphics showed no statistically significant differences between cells treated with different concentrations of EOs diluted in Dimethyl Sulfoxide (DMSO) and the corresponding concentrations of DMSO diluted in the cell culture medium.

Based on these results, it was decided to select 0.025% *v/v* as the concentration of AEO and LEO to be tested at 24 h for their potential anti-inflammatory role in the subsequent experiments. In addition, since DMSO alone did not exert a cytotoxic effect at any concentrations or time points, the following experiments were conducted excluding this experimental condition.

### 2.3. Effects of AEO and LEO on U937 Monocyte–HUVEC Interaction

The monocyte-adhesion assay was performed to assess the *in vitro* potential anti-inflammatory role of AEO and LEO on endothelial cells stimulated or not with Tumoral Necrosis Factor- $\alpha$  inflammatory cytokine (TNF- $\alpha$ , 1 ng/mL), which is useful to mimic the *in vivo* inflammatory condition. As shown in Figure 2, the pre-treatment with AEO (0.025% *v/v*) for 24 h significantly reduced the TNF- $\alpha$  stimulated U937 monocyte adhesion to both C- and GDM-HUVEC, while in basal conditions, this effect never reached statistically significant values.

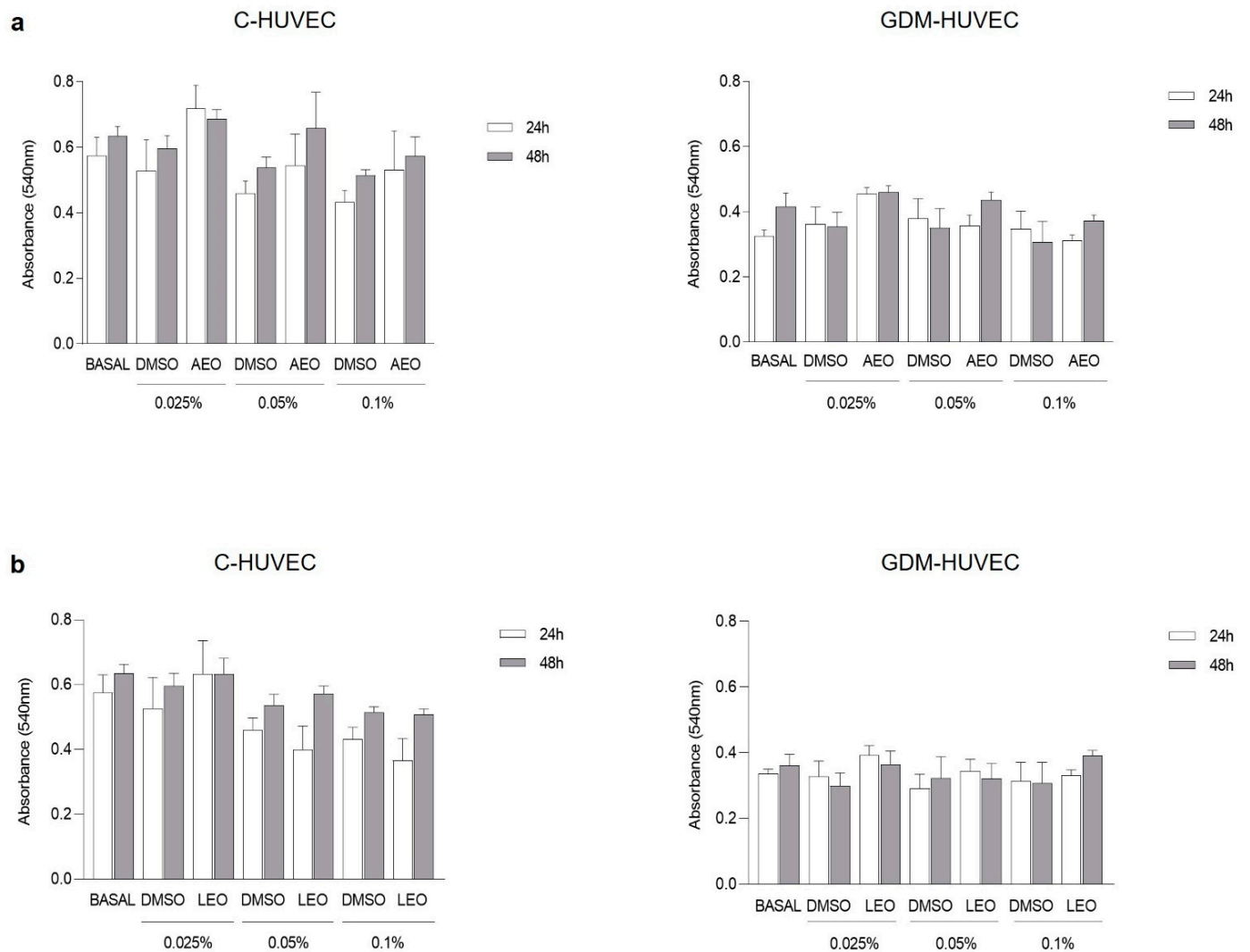


**Figure 1.** C- and GDM-HUVEC cell viability after 24 h and 48 h of treatment with (a) AEO and (b) LEO at different concentrations (0.025, 0.05, and 0.1% *v/v*) or with medium alone (BASAL). Results are shown as mean  $\pm$  Standard Error of the Mean (SEM). All experiments were conducted in technical and biological triplicate using at least 3 different primary culture strains of C- and GDM-HUVEC.

Similarly, the treatment with the same concentration of LEO for 24 h significantly decreased U937 cell adhesion to TNF- $\alpha$  stimulated C- and GDM-HUVEC (Figure 3).

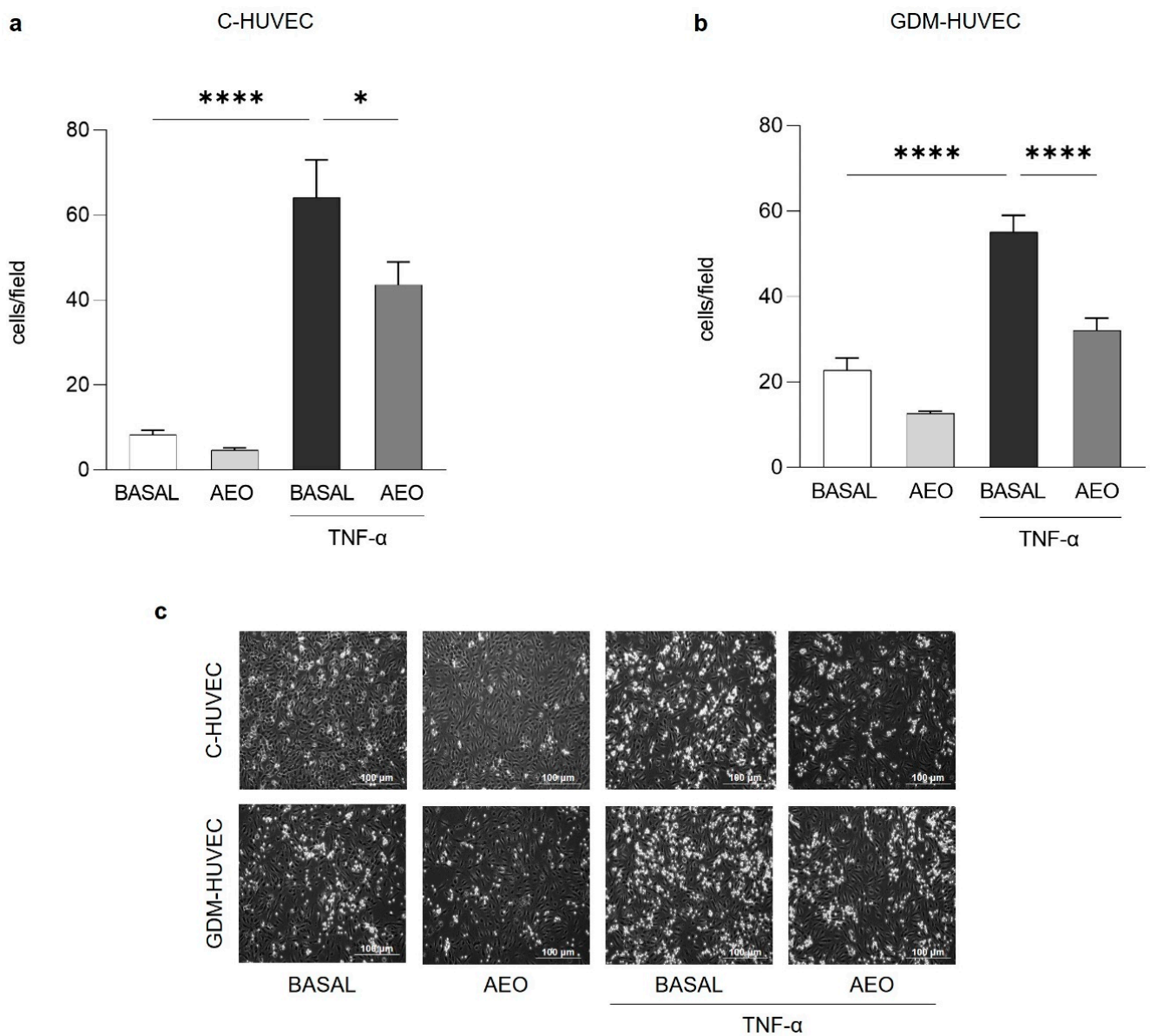


**Figure 2.** Effects of AEO on U937 monocyte adhesion to C- and GDM-HUVEC. Cells were serum-starved and incubated for 16h with TNF- $\alpha$  (1 ng/mL) following 24 h of pre-incubation with AEO (0.025% *v/v*) or with medium alone (BASAL). Quantitative data express the number of U937 cells adhering within a high-power field (3.5 mm<sup>2</sup>). Each measurement is expressed as mean  $\pm$  SEM of adhering cells from 3 independent experiments, consisting of 8 counts per condition. (a) \*\*\*\*  $p < 0.0001$  TNF- $\alpha$  vs. BASAL; \*  $p < 0.05$  TNF- $\alpha$  vs. TNF- $\alpha$  + AEO. (b) \*\*\*\*  $p < 0.0001$  TNF- $\alpha$  vs BASAL; \*\*\*\*  $p < 0.0001$  TNF- $\alpha$  vs. TNF- $\alpha$ +AEO. (c) Representative images of U937 cell adhesion to C- and GDM-HUVEC. Scale bar: 100  $\mu$ m.



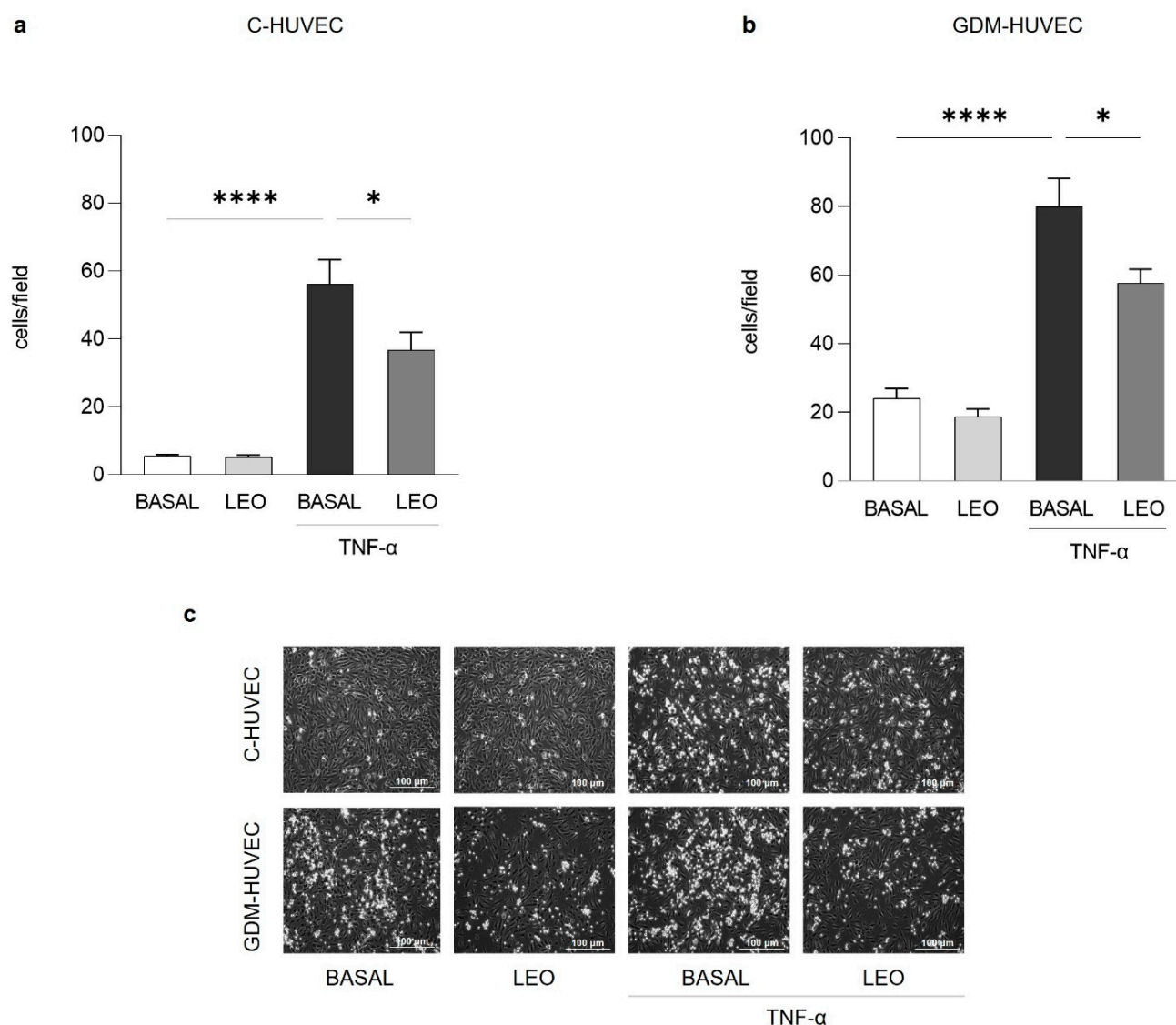


**Figure 3.** Effects of LEO on U937 monocyte adhesion to C- and GDM-HUVEC. Cells were serum-starved and incubated for 16h with TNF- $\alpha$  (1 ng/mL) following 24 h of pre-incubation with LEO (0.025% *v/v*) or with medium alone (BASAL). Quantitative data express the number of U937 cells adhering within a high-power field (3.5 mm<sup>2</sup>). Each measurement is expressed as mean  $\pm$  SEM of adhering cells from 3 independent experiments, consisting of 8 counts per condition. **(a,b)** \*\*\*\*  $p < 0.0001$  TNF- $\alpha$  vs. BASAL; \*  $p < 0.05$  TNF- $\alpha$  vs. TNF- $\alpha$ +LEO. **(c)** Representative images of U937 cell adhesion to C- and GDM-HUVEC. Scale bar: 100  $\mu$ m.

#### 2.4. Effects of AEO and LEO on VCAM-1 Membrane Exposure Levels and mRNA Expression

On the basis of the results obtained from the U937 monocyte adhesion assay and since it is well known that the vascular adhesion molecules participate in the recruitment of monocytes into the subendothelium [51], the effect of AEO and LEO on VCAM-1 membrane exposure levels was then evaluated by flow cytometry analysis.

After pre-incubating TNF- $\alpha$  stimulated cells with AEO and LEO (0.025%) for 24 h, VCAM-1 membrane exposure levels were significantly reduced in both C- (Figure 4a,c, respectively) and GDM-HUVEC (Figure 4b,d, respectively).

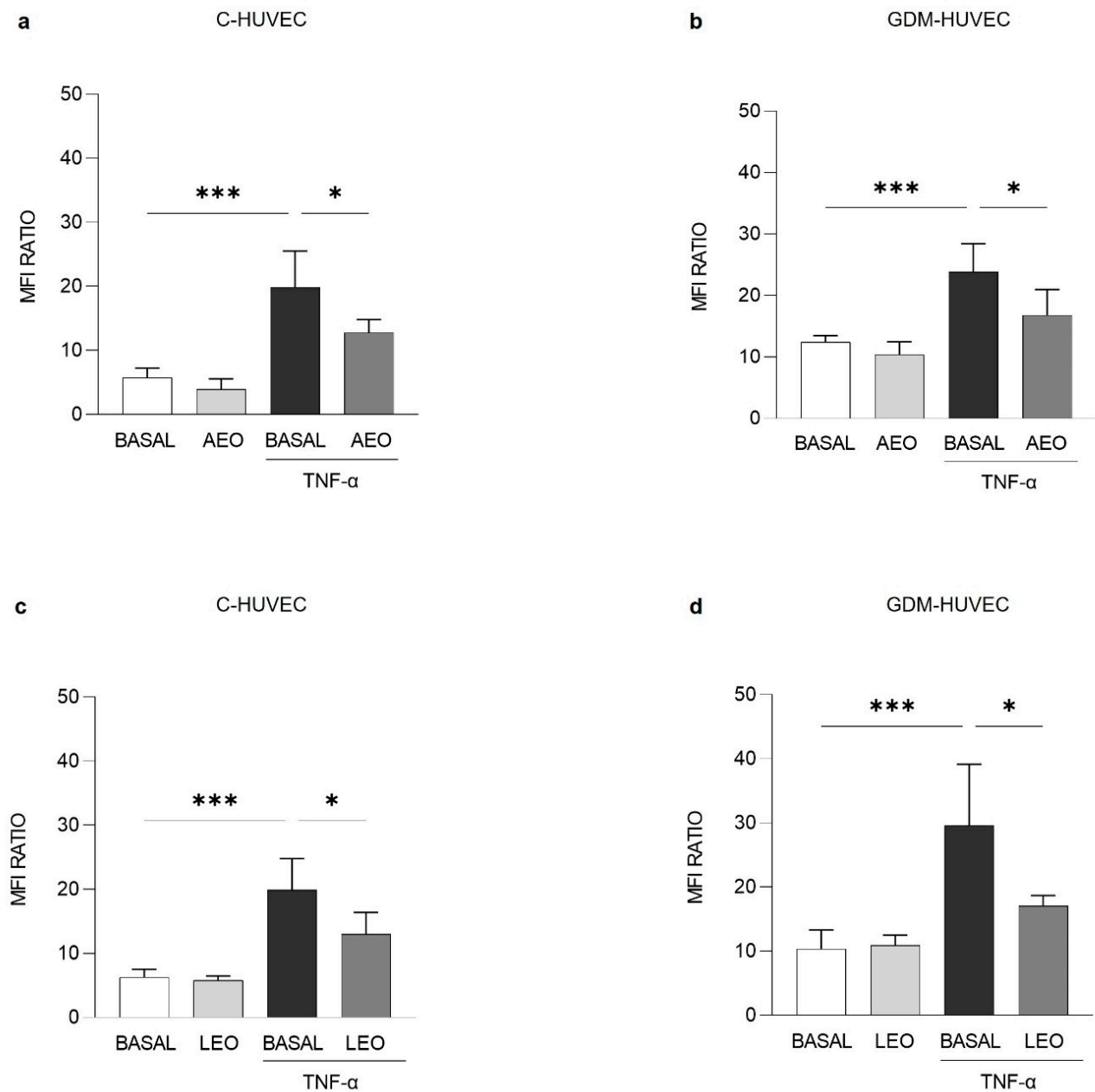


**Figure 4.** Effects of (a,b) AEO and (c,d) LEO on VCAM-1 membrane exposure levels in C- and GDM-HUVEC. Cells were serum-starved and incubated for 16h with TNF- $\alpha$  (1 ng/mL), following 24 h of pre-incubation with AEO or LEO (0.025% *v/v*) or with medium alone (BASAL). Results are presented as Mean Fluorescence Intensity (MFI) Ratio and shown as mean  $\pm$  Standard Deviation (SD). All experiments were conducted in technical and biological triplicate using at least 3 different primary culture strains of C- and GDM-HUVEC. (a–d) \*\*\*  $p < 0.001$  TNF- $\alpha$  vs. BASAL; \*  $p < 0.05$  TNF- $\alpha$  vs AEO+TNF- $\alpha$  or LEO+TNF- $\alpha$ .

Then, as shown in Figure 5, VCAM-1 mRNA expression was evaluated by Quantitative Real-Time PCR (RT-qPCR). VCAM-1 mRNA expression levels resulted in significantly reduced TNF- $\alpha$  stimulated C- and GDM-HUVEC after pre-treatment with AEO (Figure 5a,b, respectively) and LEO (Figure 5c,d, respectively).



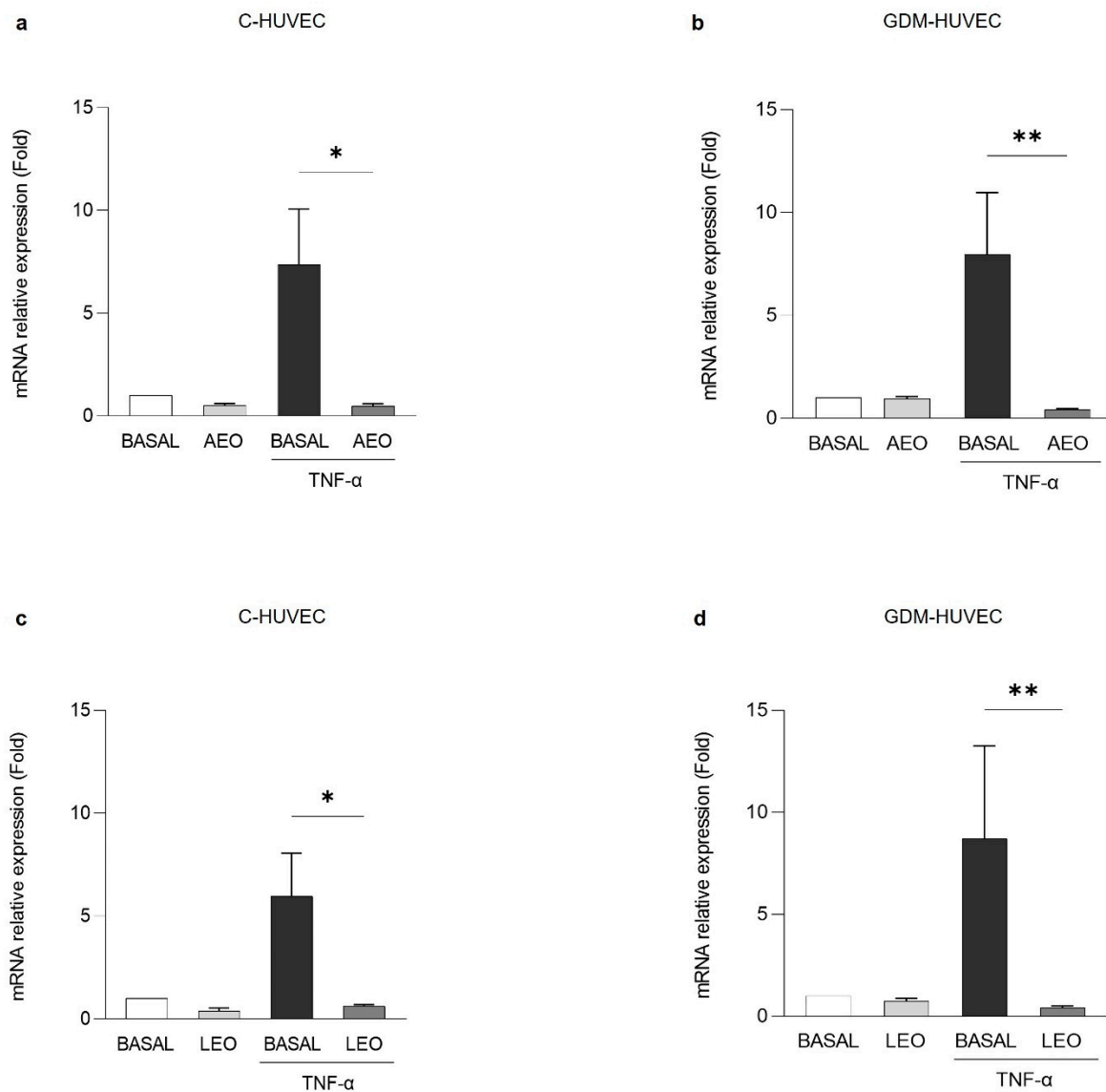


**Figure 5.** Effects of (a,b) AEO and (c,d) LEO on VCAM-1 mRNA expression in C- and GDM-HUVEC. Cells were serum-starved and incubated for 16 h with TNF- $\alpha$  (1 ng/mL), following 24 h of pre-incubation with AEO or LEO (0.025% *v/v*) or with medium alone (BASAL). Results of RT-qPCR analysis are shown as individual values and mean  $\pm$  SD of at least 3 independent experiments. (a,c) \*  $p < 0.05$  TNF- $\alpha$  vs. AEO+TNF- $\alpha$  or LEO+TNF- $\alpha$ ; (b,d) \*\*  $p < 0.01$  TNF- $\alpha$  vs. AEO+TNF- $\alpha$  or LEO+TNF- $\alpha$ .

### 2.5. Effects of AEO and LEO on NF- $\kappa$ B p65 Nuclear Translocation

NF- $\kappa$ B p65 is a nuclear transcription factor, which plays a key role in the inflammatory response [56]. In particular, the activation of the NF- $\kappa$ B signaling pathway, which occurs through its nuclear translocation, can promote the expression of vascular adhesion molecules [57]. Hence, in order to mechanistically support the potential anti-inflammatory role of AEO and LEO in C- and GDM-HUVEC, the NF- $\kappa$ B p65 activation was investigated by immunofluorescence staining.

As shown in Figures 6 and 7, both EOs (0.025% *v/v*) were able to significantly reduce TNF- $\alpha$ -induced NF- $\kappa$ B p65 cytoplasm–nucleus translocation in both C- and GDM-HUVEC, while in basal conditions, this effect reached statistical significance only in GDM-HUVEC pre-incubated with LEO (Figure 7b).

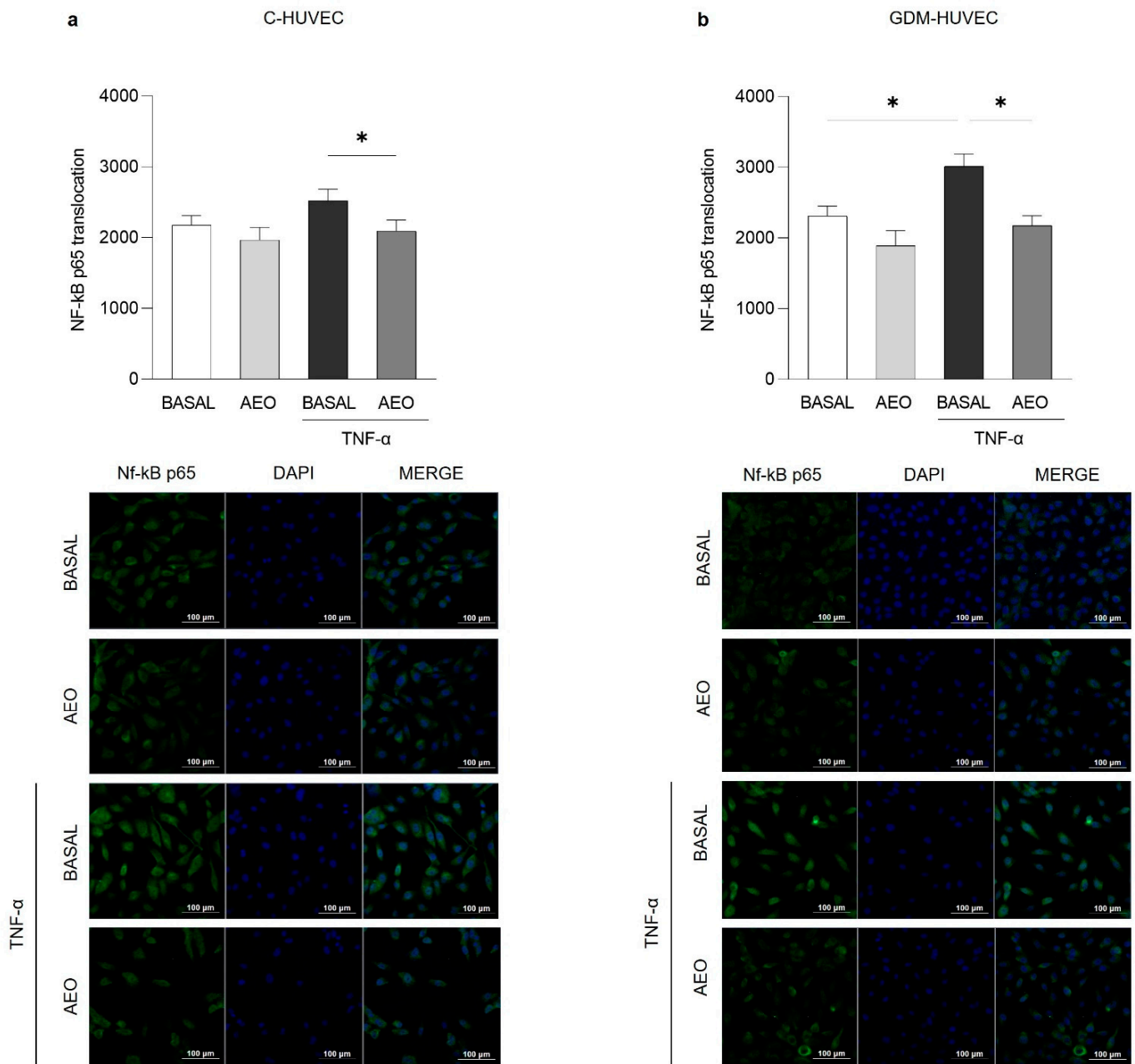


**Figure 6.** Effects of AEO on NF-κB p65 nuclear translocation in C- and GDM-HUVEC. Graphs and representative immunofluorescence images showed NF-κB p65 nuclear translocation in C- and GDM-HUVEC by immunofluorescence staining. Cells have been marked with NF-κB p65 primary antibody and Alexa Fluor 488 anti-rabbit secondary antibody, and nuclei were stained with 40, 6-diamidino-2-phenylindole (DAPI) following 24 h of treatment with AEO (0.025%). Data, calculated as the ratio of the MFI of NF-κB p65 (green) on the MFI of nuclei (blue), were obtained by analyzing at least 3 different fields for each image with ImageJ software (NIH, USA ImageJ software, public domain available at: <http://rsb.info.nih.gov/nih-image/>). Results are expressed as mean ± SEM. (a,b) \*  $p < 0.05$  TNF- $\alpha$  vs. AEO+TNF- $\alpha$ ; (b) \*  $p < 0.05$  TNF- $\alpha$  vs. BASAL. Scale bar: 100  $\mu$ m.

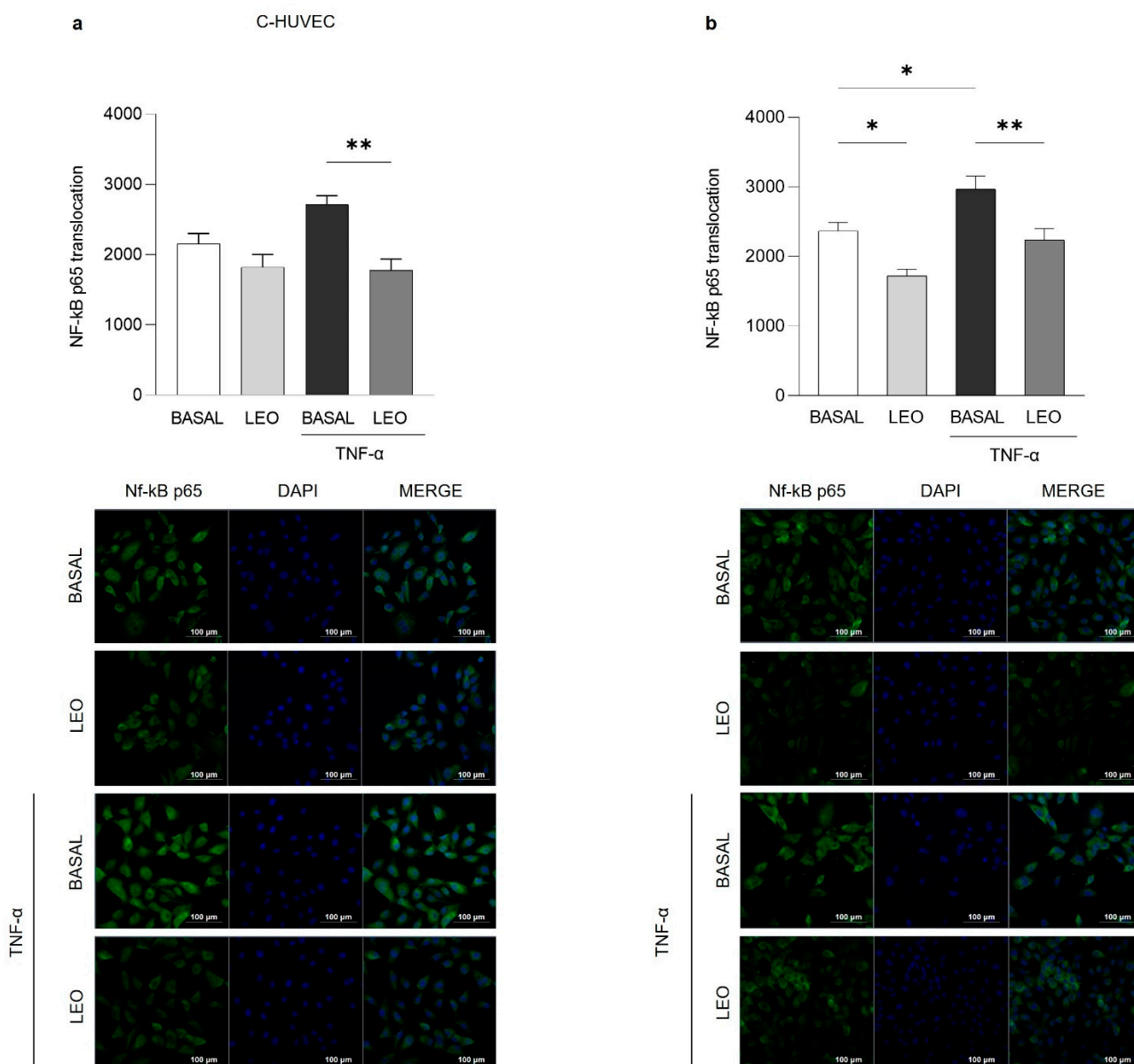


**Figure 7.** Effects of LEO on NF-κB p65 nuclear translocation in C- and GDM-HUVEC. Graphs and representative immunofluorescence images show NF-κB p65 nuclear translocation in C- and GDM-HUVEC by immunofluorescence staining. Cells have been marked with NF-κB p65 primary antibody and Alexa Fluor 488 anti-rabbit secondary antibody, and nuclei were stained with DAPI, following 24 h of treatment with LEO (0.025%). Data, calculated as the ratio of the MFI of NF-κB p65 (green) on the MFI of nuclei (blue), were obtained by analyzing at least 3 different fields for each image with ImageJ software (NIH, ImageJ software). (a,b)  $** p < 0.01$  TNF- $\alpha$  vs. LEO+TNF- $\alpha$ ; (b)  $* p < 0.05$  BASAL vs. TNF- $\alpha$  or LEO. Scale bar: 100  $\mu$ m.

### 3. Discussion

Endothelial dysfunction, associated with an increased oxidative stress and inflammatory condition, represents the first key event in the onset of vascular complications in DM [58]. Among natural bioactive compounds, the use of EOs in the moderation of inflammatory disorders nowadays represents an increasing research field [59]. In fact, EOs are showing growing interest in food and cosmetic industries, as well as in the human health field [1,26–32].

This study was based on the fact that the EOs and some of their active components have been shown to potentially exert several biological activities including modulation of various cardiovascular risk factors, such as oxidative stress and inflammation [37]. In particular, the *in vitro* use of EOs is here proposed to mitigate the burden of inflammation in vascular cells by targeting the earlier altered mechanisms involved in the onset of endothelial dysfunction.

Hence, we investigated the potential anti-inflammatory effects of AEO and LEO, which are particularly abundant in Mediterranean aromatic plants, by using GDM-HUVEC, a valuable cellular model to study the early triggering events of vascular complications associated with DM [55,60].

To this end, the potential cytotoxic effect of different concentrations of AEO and LEO on C- and GDM-HUVEC was first evaluated, demonstrating that they did not affect cell viability. Especially, the concentration of 0.025% *v/v* showed better results in terms of vitality in comparison with other concentrations used and baseline. On this basis, it was decided to perform all the subsequent tests with the use of AEO and LEO at a concentration of 0.025% *v/v* for 24 h.

Then, to investigate the possible AEO and LEO anti-inflammatory activity *in vitro*, the U937 monocyte–endothelial cell interaction rate was determined, since it is considered one of the earliest events involved in atherosclerosis [61]. After attaching to the endothelium, monocytes subsequently invade the vascular wall, where they play a central role in triggering inflammation [46,51]. Here, it was found that the stimulation with a low concentration of TNF- $\alpha$  induced an increase in the U937 monocyte–cell interaction in both cell populations. The pre-treatment with AEO, as well as LEO, significantly reduced the number of adhered U937 cells in both C- and GDM-HUVEC, even if AEO determined a stronger decrease in U937 adhesion to GDM-HUVEC with respect to LEO. On the other hand, a not significant decrease could be detected in basal conditions for both cell populations after treatment with AEO and LEO.

To further investigate this process, since it is well known that vascular adhesion molecules, such as VCAM-1, participate in the recruitment of monocytes to the endothelium [55,62,63], the effect of AEO and LEO on VCAM-1 membrane exposure levels *in vitro* was evaluated by flow cytometry analysis. After pre-incubating TNF- $\alpha$  stimulated cells with AEO and LEO for 24 h, VCAM-1 total expression and membrane exposure levels were significantly reduced in both C- and GDM-HUVEC.

Although not only VCAM-1, but also other vascular adhesion molecules, such as ICAM-1 or E-selectin, are known to be responsible for U937 cell adhesion to HUVEC [64], these data have a prominent role, considering that increased interest in the possible consumption of these compounds as support for the modulation of vascular diseases is growing. Indeed, several dietary bioactive components, although not considered essential, may hold important benefits for human health, being nowadays widely used by the food industry [34,35,38,65,66]. The efficacy of the processed product for pharmaceutical, cosmeceutical, and nutraceutical applications is directly linked to WHO guidelines on good agricultural and collection practices (WHO-GACP) and the good herbal processing (GHPP) practices, which are helpful in further enhancing the therapeutic efficacy, safety, and potential of the processed products [67,68].

Furthermore, it is well known that NF- $\kappa$ B activation can induce the transcription of a large number of genes implicated in vascular inflammation, including cytokines, chemokines, and adhesion molecules [57]. As a matter of fact, several studies performed on cells, laboratory animals, and humans have demonstrated their implication in endothelial dysfunction and atherosclerosis [69–71], both of which phenomena could be modulated by using different pharmacological or natural approaches [56,72–74]. Hence, to further investigate the potential anti-inflammatory effect of AEO and LEO on C- and GDM-HUVEC, NF- $\kappa$ B p65 activation was investigated. Interestingly, both EOs were able to significantly reduce TNF- $\alpha$ -induced NF- $\kappa$ B p65 cytoplasm–nucleus translocation in both C- and GDM-HUVEC, thus confirming the capability of AEO and LEO in reducing vascular inflammation

in vitro. Of note, NF- $\kappa$ B p65 nuclear translocation reached also statistical significance in GDM-HUVEC pre-incubated with LEO in basal conditions.

Nevertheless, several cellular studies have reported the capability of other EOs in alleviating inflammation [19,20,56,65,75], but to the best of our knowledge, this is the first report demonstrating the anti-inflammatory role of AEO and LEO in a GDM-HUVEC in vitro model.

Collectively, these findings lay the foundations for further studies in demonstrating that these EOs may help to protect human vessel endothelium from damages related to chronic hyperglycemia and type 2 DM by interfering with signal mechanisms related to vascular inflammation. These results are in line with previous in vitro and in vivo evidence based on the anti-inflammatory properties expressed by other natural bioactive compounds on HUVEC [65,75,76] and may explain some of the beneficial effects reported by the implementation of the polyphenol-rich Mediterranean diet and its related bioactive molecules [77–80].

In conclusion, the following findings reported by AEO and LEO properties in this GDM in vitro model provided evidence that these molecules may act on the vascular inflammatory state by decreasing U937 monocyte adhesion thanks to the regulation of the NF- $\kappa$ B p65 signaling pathway. This may represent another interesting mechanism to further elucidate the possible beneficial role of AEO and LEO in mitigating endothelial dysfunction.

Despite important features of these extracts that need to be improved, such as their high volatility and hydrophobicity, which could compromise their bioavailability, the information being generated by in vitro assays obviously needs to be confirmed through systematic animal studies and clinical investigations. With the help of further research, the EOs of anise and laurel could find large applications in the healthcare and nutraceutical fields, since endothelial dysfunction represents a common triggering factor of several vascular diseases.

Further studies are also required in due course on a larger number of other EOs with the purpose of establishing some quantitative composition–activity relationships (QCAR) to dissect the chemical components mainly responsible for the herein-reported biological effects.

## 4. Materials and Methods

### 4.1. Chemicals

DMSO (CAT. 102950) was purchased from Sigma-Aldrich (Merk Life Science S.r.l., Milan, Italy). TRIzol™ reagent (CAT. 15596026), High-Capacity cDNA Reverse Transcription Kit (CAT. 4368813), TaqMan Gene Expression Assays probes, and TaqManUniversal Master mix II (CAT. 4440038) were purchased from Thermo Fisher Scientific (Waltham, MA, USA).

### 4.2. GC/MS Analysis

AEO and LEO were subjected to GC/MS analysis to characterize their composition, as previously described [81]. Briefly, a Stabilwax fused-silica capillary column (Restek, Bellefonte, PA, USA) (60 m  $\times$  0.25 mm, 0.25 mm film thickness) was used and the GC oven program was as follows: isothermal exposure at 60 °C for 5 min, which was then ramped to 220 °C at a rate of 6 °C min<sup>-1</sup>, and finally, isothermal exposure at 220 °C for 20 min. The identification of components was performed by matching their mass spectra with those stored in the Wiley and NIST 02 mass spectra library databases. Furthermore, the linear retention indices (LRIs) (relative to C<sub>8</sub>–C<sub>30</sub> aliphatic hydrocarbons) were calculated and compared with available retention data presented in the literature (Nist) [82]. Relative percentages of all identified components were obtained by peak area normalization from Gas Chromatography–Flame Ionization Detection (GC-FID) chromatograms without the use of an internal standard or correction factors and expressed in percentages [10]. All analyses were repeated twice.



#### 4.3. EOs Dilution

EOs (Farmalabor srl, Assago, Italy) were dissolved in DMSO at 50 mg/mL to obtain complete solubilization, and further diluted in the medium for cell culture experiments, always resulting in a DMSO concentration that has no effect on cell viability.

#### 4.4. Cell Cultures and Experimental Protocols

Umbilical cords were collected at full-term delivery from healthy Caucasian mothers (Control, C) and those with GDM, randomly selected at Pescara Hospital (Pescara, Italy). All procedures were performed in agreement with the ethical standards of the Institutional Committee on Human Experimentation (Reference Number: 1879/09COET) and with the Declaration of Helsinki Principles. Informed consent was signed by each participating subject after approval of the protocol by the Institutional Review Board.

Primary C- and GDM-HUVEC were obtained, cultured (5% CO<sub>2</sub> and 37 °C), and used between the 3rd and 5th passages in vitro, as previously described [83].

After that, HUVEC were grown to sub-confluence in complete Cell Culture Media–Dulbecco’s Modification of Eagle’s Medium (DMEM, CAT. 10014CV, Corning™, Glendale, AZ, USA), M199 with Earle’s salts and L-glutamine (CAT. 10060CV, Corning™, Glendale, AZ, USA), L-glutamine (CAT. 25005CL, Corning™, Glendale, AZ, USA), Penicillin-Streptomycin (CAT. P0607100, Corning™, Glendale, AZ, USA), and Fetal Bovine Serum (FBS, CAT. 41A0045K, Gibco-Life Technologies, Thermo Fisher Scientific, Waltham, MA, USA) for all the following experimental tests.

First of all, the potential cytotoxic effect of AEO and LEO, extracted from the related Mediterranean plants, was evaluated in order to find the most suitable EO concentration to perform all the subsequent experiments. For this aim, C- and GDM-HUVEC were stimulated for 24 h and 48 h with different concentrations of oils (0.025%, 0.05%, and 0.1% *v/v*) dissolved in DMSO. Then, cell viability was evaluated.

The obtained results allowed us to select the best AEO and LEO concentrations (0.025% *v/v*) to test for their potential anti-inflammatory role. For this purpose, in each experiment, C- and GDM-HUVEC were serum-starved (with 0.1% FBS) and incubated for 16h with TNF- $\alpha$  (1 ng/mL, CAT. PHC3015L, Gibco-Life Technologies, Thermo Fisher Scientific, Waltham, MA, USA), following 24 h of pre-incubation with AEO and LEO, or with medium alone as a basal condition.

#### 4.5. MTT Assay

The effect of AEO and LEO on C- and GDM-HUVEC viability was assessed by the MTT (Sigma-Aldrich, Merk Life Science S.r.l., Milan, Italy) assay according to the manufacturer’s instructions.

Cells were seeded into 96-well plates, grown to confluence, and stimulated for 24 h and 48 h with different EO concentrations dissolved in DMSO: 0.025%, 0.05%, and 0.1% *v/v*, or with DMSO and the medium alone as controls. Briefly, after 24 h and 48 h of treatment, a solution of diluted MTT in phosphate buffer (PBS; Sigma Aldrich, Merk Life Science S.r.l., Milan, Italy) was added to each well at a concentration of 0.5 mg/mL. Following 3 h of incubation at 37 °C, 0.2 mL of DMSO per well was added for 30 min. Then, cell viability was evaluated by measuring the spectrometric absorbance (ABS) at a 540 nm wavelength using a microplate reader (SpectraMAX 190, Molecular Devices Inc., Sunnyvale, CA, USA).

#### 4.6. U937 Monocyte Adhesion Assay

The adhesion of the human monocyte line U937 to C- and GDM-HUVEC was evaluated in a basal state, after 16h of TNF- $\alpha$  (1 ng/mL) exposure, and in presence of AEO and LEO (after 24 h of pre-incubation) alone or in combination with TNF- $\alpha$ , as described in Section 4.4. U937 monocyte cell suspensions were added to each HUVEC monolayer under rotating conditions at room temperature (RT) and the assay was performed as previously described [76].



#### 4.7. Flow Cytometry Analysis

The levels of VCAM-1 protein membrane exposure were evaluated using the flow cytometry analysis.

Briefly, cells were detached by 0.5% trypsin/0.2% EDTA solution (CAT. 59418C, Sigma-Aldrich, Milan, Italy), collected with PBS, and resuspended in Bovine Serum Albumin (BSA 0.5%, CAT. PR23225, Euroclone, Milan, Italy). Then, they were centrifugated at 800 rpm for 15 min at 4 °C. After that, cells were incubated with PE-labelled anti-VCAM-1 antibody (1:20, CAT. 305806, BioLegend, San Diego, CA, USA) for 30 min at RT.

All data were analyzed using FACS Diva (BD Biosciences, San Diego, CA, USA) and FlowJo v.8.8.6 software (TreeStar, Ashland, OR, USA) and expressed as MFI Ratio. The MFI Ratio was calculated by dividing the MFI of positive events by the MFI of negative events (MFI of the secondary antibody).

#### 4.8. RTq-PCR

The total RNA was isolated and extracted from HUVEC using the TRIzol™ reagent protocol, then the High-Capacity cDNA Reverse Transcription Kit was employed to synthesize cDNA.

The TaqMan Universal Master Mix II and TaqMan Gene Expression Assay probes for human VCAM-1 (Hs01003372\_m1) and GAPDH (Hs02786624\_g1) were used according to the manufacturer's instructions. Gene expression was assessed with the ABI Prism 7900 Sequence Detection System (ThermoFisher Scientific, Waltham, MA, USA). The relative gene expression was calculated using the comparative  $2^{-\Delta\Delta CT}$  method and results are expressed as the fold change related to the untreated control.

#### 4.9. NF- $\kappa$ B p65 Evaluation by Immunofluorescence

NF- $\kappa$ B p65 nuclear translocation in C- and GDM-HUVEC was assessed by immunofluorescence staining.

Cells were treated with AEO and LEO (0.025% *v/v*) for 24 h and then stimulated with TNF- $\alpha$  for 2 h to evaluate NF- $\kappa$ B cytoplasm–nucleus translocation. The assay was performed on C- and GDM-HUVEC seeded in a Chamber Polystyrene Vessel Tissue Culture Treated Glass Slide (BD Falcon, Franklin Lakes, NJ, USA) (30,000 cells/chamber). After 24 h of treatment, cells were fixed with 3% Paraformaldehyde (10 min at RT), permeabilized with a solution (HEPES 20 mM pH 7.4, saccharose 300  $\mu$ M, NaCl 50 mM, MgCl<sub>2</sub> 3 mM, and Triton X-100 0.5%), and incubated with NF- $\kappa$ B p65 primary antibody (1:50, overnight at 4 °C, CAT. P65C2284, Cell Signaling Technology, Milan, Italy) and Alexa Fluor 488 anti-rabbit secondary antibody (1:50, 30 min at RT, CAT. A11034, Invitrogen, Thermo Fisher Scientific, Waltham, MA, USA). Lastly, the nuclei were stained with DAPI (1:5000, 15 min at RT, CAT. D9542, Sigma-Aldrich, Merk Life Science S.r.l., Milan, Italy) and then observed using a confocal microscope (Zeiss LSM-800, Carl Zeiss Meditec AG, Oberkochen, Germany).

Data were expressed as the ratio of the MFI of NF- $\kappa$ B p65 (green) on the MFI of nuclei (blue) by analyzing at least 3 different fields for each image with ImageJ software (NIH, ImageJ software).

#### 4.10. Statistical Analysis

All experimental data are presented as mean  $\pm$  SD or SEM. All experiments were conducted in technical and biological triplicate using at least 3 different primary culture strains of C- and GDM-HUVEC.

Statistical analysis was performed using One-Way Analysis of Variance (ANOVA), Bonferroni multiple comparison test for post hoc comparison, and the Kruskal–Wallis or Dunn's post hoc tests. *p*-values < 0.05 were considered statistically significant. Analysis and graphs were performed using GraphPad Prism Software Analysis (version 9).

**Author Contributions:** Conceptualization, N.D.P. (Natalia Di Pietro) and R.R.; methodology, V.S., T.R., C.P. (Carola Palmerini), S.G., M.P.A.B. and P.D.T.; software, D.M. and R.R.; validation, N.D.P. (Natalia Di Pietro) and R.R.; formal analysis, V.S., D.M. and N.D.P. (Nadia Di Pietrantonio); investigation, V.S., T.R. and C.P. (Carola Palmerini); resources, A.P. and R.R.; data curation, N.D.P. (Natalia Di Pietro), R.R., and A.P.; writing—original draft preparation N.D.P. (Natalia Di Pietro), R.R., V.S. and T.R.; writing—review and editing N.D.P. (Natalia Di Pietro), C.P. (Caterina Pipino) and A.P.; visualization, E.B., R.F. and M.S.; supervision, N.D.P. (Natalia Di Pietro); project administration, N.D.P. (Natalia Di Pietro) and R.R. All authors have read and agreed to the published version of the manuscript.

**Funding:** This research received no external funding.

**Institutional Review Board Statement:** Not applicable.

**Informed Consent Statement:** Not applicable.

**Data Availability Statement:** Not applicable.

**Conflicts of Interest:** The authors declare no conflict of interest.

## References

1. Kapadia, P.; Newell, A.S.; Cunningham, J.; Roberts, M.R.; Hardy, J.G. Extraction of High-Value Chemicals from Plants for Technical and Medical Applications. *Int. J. Mol. Sci.* **2022**, *23*, 10334. [[CrossRef](#)]
2. Božović, M.; Navarra, A.; Garzoli, S.; Pepi, F.; Ragno, R. Essential Oils Extraction: A 24-Hour Steam Distillation Systematic Methodology. *Nat. Prod. Res.* **2017**, *31*, 2387–2396. [[CrossRef](#)] [[PubMed](#)]
3. Raut, J.S.; Karuppaiyil, S.M. A Status Review on the Medicinal Properties of Essential Oils. *Ind. Crops Prod.* **2014**, *62*, 250–264. [[CrossRef](#)]
4. Thalappil, M.A.; Butturini, E.; Carcereri de Prati, A.; Bettin, I.; Antonini, L.; Sapienza, F.U.; Garzoli, S.; Ragno, R.; Mariotto, S. Pinus Mugo Essential Oil Impairs STAT3 Activation through Oxidative Stress and Induces Apoptosis in Prostate Cancer Cells. *Molecules* **2022**, *27*, 4834. [[CrossRef](#)] [[PubMed](#)]
5. Machado, T.Q.; da Fonseca, A.C.C.; Duarte, A.B.S.; Robbs, B.K.; de Sousa, D.P. A Narrative Review of the Antitumor Activity of Monoterpenes from Essential Oils: An Update. *BioMed Res. Int.* **2022**, *2022*, 6317201. [[CrossRef](#)]
6. Sabatino, M.; Fabiani, M.; Božović, M.; Garzoli, S.; Antonini, L.; Marocci, M.E.; Palamara, A.T.; de Chiara, G.; Ragno, R. Molecules Experimental Data Based Machine Learning Classification Models with Predictive Ability to Select in Vitro Active Antiviral and Non-Toxic Essential Oils. *Molecules* **2020**, *25*, 2452. [[CrossRef](#)]
7. Zhang, Y.; Li, X.Y.; Zhang, B.S.; Ren, L.N.; Lu, Y.P.; Tang, J.W.; Lv, D.; Yong, L.; Lin, L.T.; Lin, Z.X.; et al. In Vivo Antiviral Effect of Plant Essential Oils against Avian Infectious Bronchitis Virus. *BMC Vet. Res.* **2022**, *18*, 1–13. [[CrossRef](#)]
8. Madaia, V.N.; Toscanelli, W.; de Vita, D.; de Angelis, M.; Messore, A.; Ialongo, D.; Scipione, L.; Tudino, V.; D'auria, F.D.; di Santo, R.; et al. Ultrastructural Damages to H1N1 Influenza Virus Caused by Vapor Essential Oils. *Molecules* **2022**, *27*, 3718. [[CrossRef](#)]
9. Schnitzler, P. Essential Oils for the Treatment of Herpes Simplex Virus Infections. *Chemotherapy* **2019**, *64*, 1–7. [[CrossRef](#)]
10. Oliva, A.; Costantini, S.; de Angelis, M.; Garzoli, S.; Božović, M.; Mascellino, M.T.; Vullo, V.; Ragno, R. High Potency of Melaleuca Alternifolia Essential Oil against Multi-Drug Resistant Gram-Negative Bacteria and Methicillin-Resistant Staphylococcus Aureus. *Molecules* **2018**, *23*, 2584. [[CrossRef](#)]
11. Alibi, S.; Ben, S.W.; Mansour, H.B.; Navas, J. Activity of Essential Oils Against Multidrug-Resistant Salmonella Enteritidis. *Curr. Microbiol.* **2022**, *79*, 1–10. [[CrossRef](#)]
12. Razzouk, S.; Mazri, M.A.; Jeldi, L.; Mnasri, B.; Ouahmane, L.; Alfeddy, M.N. Chemical Composition and Antimicrobial Activity of Essential Oils from Three Mediterranean Plants against Eighteen Pathogenic Bacteria and Fungi. *Pharmaceutics* **2022**, *14*, 1608. [[CrossRef](#)]
13. Sienkiewicz, M.; Głowacka, A.; Poznańska-Kurowska, K.; Kaszuba, A.; Urbaniak, A.; Kowalczyk, E. Original Paper<br>The Effect of Clary Sage Oil on Staphylococci Responsible for Wound Infections. *Adv. Dermatol. Allergol. Postępy Dermatol. I Alergol.* **2015**, *32*, 21–26. [[CrossRef](#)]
14. Chelaghema, A.; Durand, N.; Servent, A.; Mamouni, M.; Pouchet, P.; Schorr-Galindo, S.; Fontana, A.; Strub, C. Antifungal and Antimycotoxic Activities of 3 Essential Oils against 3 Mycotoxinogenic Fungi. *Arch. Microbiol.* **2022**, *204*, 1–16. [[CrossRef](#)]
15. Parker, R.A.; Gabriel, K.T.; Graham, K.D.; Butts, B.K.; Cornelison, C.T. Antifungal Activity of Select Essential Oils against Candida Auris and Their Interactions with Antifungal Drugs. *Pathogens* **2022**, *11*, 821. [[CrossRef](#)] [[PubMed](#)]
16. Artini, M.; Papa, R.; Sapienza, F.; Božović, M.; Vrenna, G.; Assanti, V.T.G.; Sabatino, M.; Garzoli, S.; Fiscarelli, E.V.; Ragno, R.; et al. Essential Oils Biofilm Modulation Activity and Machine Learning Analysis on Pseudomonas Aeruginosa Isolates from Cystic Fibrosis Patients. *Microorganisms* **2022**, *10*, 887. [[CrossRef](#)] [[PubMed](#)]
17. Jeong, Y.J.; Kim, H.E.; Han, S.J.; Choi, J.S. Antibacterial and Antibiofilm Activities of Cinnamon Essential Oil Nanoemulsion against Multi-Species Oral Biofilms. *Sci. Rep.* **2021**, *11*, 1–8. [[CrossRef](#)] [[PubMed](#)]

18. Morshdy, A.E.M.A.; El-Tahlawy, A.S.; Qari, S.H.; Qumsani, A.T.; Bay, D.H.; Sami, R.; Althubaiti, E.H.; Mansour, A.M.A.; Aljahani, A.H.; Hafez, A.E.S.E.; et al. Anti-Biofilms' Activity of Garlic and Thyme Essential Oils against Salmonella Typhimurium. *Molecules* **2022**, *27*, 2182. [[CrossRef](#)]
19. Pandur, E.; Micalizzi, G.; Mondello, L.; Horváth, A.; Sipos, K.; Horváth, G. Antioxidant and Anti-Inflammatory Effects of Thyme (*Thymus Vulgaris* L.) Essential Oils Prepared at Different Plant Phenophases on Pseudomonas Aeruginosa LPS-Activated THP-1 Macrophages. *Antioxidants* **2022**, *11*, 1330. [[CrossRef](#)]
20. Li, C.; Cai, Q.; Wu, X.; Tan, Z.; Yao, L.; Huang, S.; Zhang, W.; Hong, Z.; Chen, Z.; Zhang, L. Anti-Inflammatory Study on the Constituents of Angelica Sinensis (Oliv.) Diels, Angelica Dahurica (Hoffm.) Benth. & Hook.f. Ex Franch. & Sav., Angelica Pubescence Maxim and Foeniculum Vulgare Mill. Essential Oils. *J. Oleo Sci.* **2022**, *71*, 1207–1219. [[CrossRef](#)]
21. Padilla-Camberos, E.; Sanchez-Hernandez, I.M.; Torres-Gonzalez, O.R.; Gallegos-Ortiz, M.R.; Méndez-Mona, A.L.; Baez-Moratilla, P.; Flores-Fernandez, J.M. Natural Essential Oil Mix of Sweet Orange Peel, Cumin, and Allspice Elicits Anti-Inflammatory Activity and Pharmacological Safety Similar to Non-Steroidal Anti-Inflammatory Drugs. *Saudi J. Biol. Sci.* **2022**, *29*, 3830–3837. [[CrossRef](#)]
22. Fan, H.; Zhang, L.; Li, Y.; Soo Khoo, C.; Han, D.; Liu, Q.; Li, P.; Zhang, X. Antioxidant and Immunomodulatory Activities of Essential Oil Isolated from Anti-Upper Respiratory Tract Infection Formulation and Their Chemical Analysis. *Evid. Based Complement. Altern. Med.* **2022**, *2022*, 1–9. [[CrossRef](#)]
23. Ferreira, O.O.; Cruz, J.N.; de Moraes, A.B.; Franco, C.D.J.P.; Lima, R.R.; dos Anjos, T.O.; Siqueira, G.M.; Nascimento, L.D.D.; Cascaes, M.M.; de Oliveira, M.S.; et al. Essential Oil of the Plants Growing in the Brazilian Amazon: Chemical Composition, Antioxidants, and Biological Applications. *Molecules* **2022**, *27*, 4373. [[CrossRef](#)]
24. Minchán-Herrera, P.; Ybañez-Julca, R.O.; Quispe-Díaz, I.M.; Venegas-Casanova, E.A.; Jara-Aguilar, R.; Salas, F.; Zevallos-Escobar, L.; Yáñez, O.; Pino-Rios, R.; Calderon, P.B.; et al. Valeriana Pilosa Roots Essential Oil: Chemical Composition, Antioxidant Activities, and Molecular Docking Studies on Enzymes Involved in Redox Biological Processes. *Antioxidants* **2022**, *11*, 1337. [[CrossRef](#)]
25. de Lavor, É.M.; Fernandes, A.W.C.; de Andrade Teles, R.B.; Leal, A.E.B.P.; de Oliveira, R.G., Jr.; Silva, M.G.; de Oliveira, A.P.; Silva, J.C.; de Moura Fontes Araújo, M.T.; Coutinho, H.D.M.; et al. Essential Oils and Their Major Compounds in the Treatment of Chronic Inflammation: A Review of Antioxidant Potential in Preclinical Studies and Molecular Mechanisms. *Oxid. Med. Cell. Longev.* **2018**, *2018*, 1–23. [[CrossRef](#)]
26. Shiina, Y.; Funabashi, N.; Lee, K.; Toyoda, T.; Sekine, T.; Honjo, S.; Hasegawa, R.; Kawata, T.; Wakatsuki, Y.; Hayashi, S.; et al. Relaxation Effects of Lavender Aromatherapy Improve Coronary Flow Velocity Reserve in Healthy Men Evaluated by Transthoracic Doppler Echocardiography. *Int. J. Cardiol.* **2008**, *129*, 193–197. [[CrossRef](#)]
27. Lai, T.K.T.; Cheung, M.C.; Lo, C.K.; Ng, K.L.; Fung, Y.H.; Tong, M.; Yau, C.C. Effectiveness of Aroma Massage on Advanced Cancer Patients with Constipation: A Pilot Study. *Complement. Clin. Pr.* **2011**, *17*, 37–43. [[CrossRef](#)]
28. Atsumi, T.; Tonosaki, K. Smelling Lavender and Rosemary Increases Free Radical Scavenging Activity and Decreases Cortisol Level in Saliva. *Psychiatry Res.* **2007**, *150*, 89–96. [[CrossRef](#)]
29. Carson, C.F.; Smith, D.W.; Lampacher, G.J.; Riley, T.V. Use of Deception to Achieve Double-Blinding in a Clinical Trial of Melaleuca Alternifolia (Tea Tree) Oil for the Treatment of Recurrent Herpes Labialis. *Contemp. Clin. Trials* **2008**, *29*, 9–12. [[CrossRef](#)]
30. Marchand, L. Integrative and Complementary Therapies for Patients with Advanced Cancer. *Ann. Palliat. Med.* **2014**, *3*, 16071–16171. [[CrossRef](#)]
31. Abbasjahromi, A.; Hojati, H.; Nikooei, S.; Jahromi, H.K.; Dowlatkhan, H.R.; Zarean, V.; Farzaneh, M.; Kalavani, A. Compare the Effect of Aromatherapy Using Lavender and Damask Rose Essential Oils on the Level of Anxiety and Severity of Pain Following C-Section: A Double-Blinded Randomized Clinical Trial. *J. Complement. Integr. Med.* **2020**, *17*, 31730539. [[CrossRef](#)] [[PubMed](#)]
32. Zhang, Y.; Long, Y.; Yu, S.; Li, D.; Yang, M.; Guan, Y.; Zhang, D.; Wan, J.; Liu, S.; Shi, A.; et al. Natural Volatile Oils Derived from Herbal Medicines: A Promising Therapy Way for Treating Depressive Disorder. *Pharm. Res.* **2021**, *164*, 105376. [[CrossRef](#)] [[PubMed](#)]
33. Zhao, C.; Cao, Y.; Zhang, Z.; Nie, D.; Li, Y. Cinnamon and Eucalyptus Oils Suppress the Inflammation Induced by Lipopolysaccharide In Vivo. *Molecules* **2021**, *26*, 7410. [[CrossRef](#)] [[PubMed](#)]
34. De Blasio, A.; D'Anneo, A.; Lauricella, M.; Emanuele, S.; Giuliano, M.; Pratelli, G.; Calvaruso, G.; Carlisi, D. The Beneficial Effects of Essential Oils in Anti-Obesity Treatment. *Int. J. Mol. Sci.* **2021**, *22*, 11832. [[CrossRef](#)]
35. Leherbauer, I.; Stappen, I. Selected Essential Oils and Their Mechanisms for Therapeutic Use against Public Health Disorders. An Overview. *Z. Für Nat. Sect. C J. Biosci.* **2020**, *75*, 205–223. [[CrossRef](#)]
36. Edris, A.E. Pharmaceutical and Therapeutic Potentials of Essential Oils and Their Individual Volatile Constituents: A Review. *Phytother. Res.* **2007**, *21*, 308–323. [[CrossRef](#)]
37. Long, Y.; Li, D.; Yu, S.; Zhang, Y.L.; Liu, S.Y.; Wan, J.Y.; Shi, A.; Deng, J.; Wen, J.; Li, X.Q.; et al. Natural Essential Oils: A Promising Strategy for Treating Cardio-Cerebrovascular Diseases. *J. Ethnopharmacol.* **2022**, *297*, 115421. [[CrossRef](#)]
38. Rajeshwari, U.; Shobha, I.; Andallu, B. Comparison of Aniseeds and Coriander Seeds for Antidiabetic, Hypolipidemic and Antioxidant Activities. *Spatula DD Peer Rev. J. Complement. Med. Drug Discov.* **2011**, *1*, 9. [[CrossRef](#)]
39. Alqahtani, Y.S.; Mahnashi, M.H.; Alyami, B.A.; Alqarni, A.O.; Huneif, M.A.; Nahari, M.H.; Ali, A.; Javed, Q.; Ilyas, H.; Rafiq, M. Preparation of Spice Extracts: Evaluation of Their Phytochemical, Antioxidant, Antityrosinase, and Anti- $\alpha$ -Glucosidase Properties Exploring Their Mechanism of Enzyme Inhibition with Antibrowning and Antidiabetic Studies In Vivo. *BioMed Res. Int.* **2022**, *2022*, 9983124. [[CrossRef](#)]

40. Mohammed, R.R.; Omer, A.K.; Yener, Z.; Uyar, A.; Ahmed, A.K. Biomedical Effects of *Laurus Nobilis* L. Leaf Extract on Vital Organs in Streptozotocin-Induced Diabetic Rats: Experimental Research. *Ann. Med. Surg.* **2020**, *61*, 188–197. [[CrossRef](#)]
41. Khan, A.; Zaman, G.; Anderson, R.A. Bay Leaves Improve Glucose and Lipid Profile of People with Type 2 Diabetes. *J. Clin. Biochem. Nutr.* **2009**, *44*, 52–56. [[CrossRef](#)]
42. Chbili, C.; Maoua, M.; Selmi, M.; Mrad, S.; Khairi, H.; Limem, K.; Mrizek, N.; Saguem, S.; Ben Fredj, M. Evaluation of Daily *Laurus Nobilis* Tea Consumption on Lipid Profile Biomarkers in Healthy Volunteers. *J. Am. Coll. Nutr.* **2020**, *39*, 733–738. [[CrossRef](#)]
43. Iftikhar, N.; Hussain, A.I.; Kamal, G.M.; Manzoor, S.; Fatima, T.; Alswailmi, F.K.; Ahmad, A.; Alsuwayt, B.; Abdullah Alnasser, S.M. Antioxidant, Anti-Obesity, and Hypolipidemic Effects of Polyphenol Rich Star Anise (*Illicium Verum*) Tea in High-Fat-Sugar Diet-Induced Obesity Rat Model. *Antioxidants* **2022**, *11*, 2240. [[CrossRef](#)]
44. Basak, S.S.; Candan, F. Effect of *Laurus Nobilis* L. Essential Oil and Its Main Components on  $\alpha$ -Glucosidase and Reactive Oxygen Species Scavenging Activity. *Shaheed Beheshti Univ. Med. Sci. Health Serv. Iran. J. Pharm. Res.* **2013**, *12*, 367–379.
45. Casamassima, D.; Palazzo, M.; Vizzarri, F.; Coppola, R.; Costagliola, C.; Corino, C.; Di Costanzo, A. Dietary Effect of Dried Bay Leaves (*Laurus Nobilis*) Meal on Some Biochemical Parameters and on Plasma Oxidative Status in New Zealand White Growing Rabbit. *J. Anim. Physiol. Anim. Nutr.* **2017**, *101*, e175–e184. [[CrossRef](#)]
46. Pandolfi, A.; De Filippis, E.A. Chronic Hyperglycemia and Nitric Oxide Bioavailability Play a Pivotal Role in Pro-Atherogenic Vascular Modifications. *Genes Nutr.* **2007**, *2*, 195–208. [[CrossRef](#)]
47. Zhu, Y.P.; Shen, T.; Lin, Y.J.; Chen, B.D.; Ruan, Y.; Cao, Y.; Qiao, Y.; Man, Y.; Wang, S.; Li, J. Astragalus Polysaccharides Suppress ICAM-1 and VCAM-1 Expression in TNF- $\alpha$ -Treated Human Vascular Endothelial Cells by Blocking NF-KB Activation. *Acta Pharm. Sin.* **2013**, *34*, 1036–1042. [[CrossRef](#)]
48. Huang, N.; Xu, Y.; Zhou, H.; Lin, D.; Zhang, B.; Zhang, Y.; Pan, D.; Tao, L.; Liu, X.; Shen, X. Essential Oil from Fructus *Alpiniae Zerumbet* Protects Human Umbilical Vein Endothelial Cells In Vitro from Injury Induced by High Glucose Levels by Suppressing Nuclear Transcription Factor-Kappa B Signaling. *Med. Sci. Monit.* **2017**, *23*, 4760–4767. [[CrossRef](#)]
49. Csiszar, A.; Wang, M.; Lakatta, E.G.; Ungvari, Z. Inflammation and Endothelial Dysfunction during Aging: Role of NF-KappaB. *J. Appl. Physiol.* **2008**, *105*, 1333–1341. [[CrossRef](#)]
50. Li, H.; Cybulsky, M.I.; Gimbrone, M.A.; Libby, P. An Atherogenic Diet Rapidly Induces VCAM-1, a Cytokine-Regulatable Mononuclear Leukocyte Adhesion Molecule, in Rabbit Aortic Endothelium. *Arter. Thromb.* **1993**, *13*, 197–204. [[CrossRef](#)]
51. Libby, P.; Ridker, P.M.; Maseri, A. Inflammation and Atherosclerosis. *Circulation* **2002**, *105*, 1135–1143. [[CrossRef](#)] [[PubMed](#)]
52. Parrettini, S.; Caroli, A.; Torlone, E. Nutrition and Metabolic Adaptations in Physiological and Complicated Pregnancy: Focus on Obesity and Gestational Diabetes. *Front. Endocrinol.* **2020**, *11*, 611929. [[CrossRef](#)] [[PubMed](#)]
53. Simeoni, U.; Barker, D.J. Offspring of Diabetic Pregnancy: Long-Term Outcomes. *Semin. Fetal Neonatal Med.* **2009**, *14*, 119–124. [[CrossRef](#)] [[PubMed](#)]
54. Di Pietrantonio, N.; Palmerini, C.; Pipino, C.; Baldassarre, M.P.A.; Bologna, G.; Mohn, A.; Giannini, C.; Lanuti, P.; Chiarelli, F.; Pandolfi, A.; et al. Plasma from Obese Children Increases Monocyte-Endothelial Adhesion and Affects Intracellular Insulin Signaling in Cultured Endothelial Cells: Potential Role of MTORC1-S6K1. *Biochim. Biophys. Acta Mol. Basis Dis.* **2021**, *1867*, 166076. [[CrossRef](#)]
55. Di Fulvio, P.; Pandolfi, A.; Formoso, G.; Di Silvestre, S.; Di Tomo, P.; Giardinelli, A.; De Marco, A.; Di Pietro, N.; Taraborrelli, M.; Sancilio, S.; et al. Features of Endothelial Dysfunction in Umbilical Cord Vessels of Women with Gestational Diabetes. *Nutr. Metab. Cardiovasc. Dis.* **2014**, *24*, 1337–1345. [[CrossRef](#)]
56. Di Tomo, P.; Canali, R.; Ciavardelli, D.; Di Silvestre, S.; De Marco, A.; Giardinelli, A.; Pipino, C.; Di Pietro, N.; Virgili, F.; Pandolfi, A.  $\beta$ -Carotene and Lycopene Affect Endothelial Response to TNF- $\alpha$  Reducing Nitro-Oxidative Stress and Interaction with Monocytes. *Mol. Nutr. Food Res.* **2012**, *56*, 217–227. [[CrossRef](#)]
57. Chen, C.C.; Manning, A.M. Transcriptional Regulation of Endothelial Cell Adhesion Molecules: A Dominant Role for NF-Kappa B. *Agents Actions Suppl.* **1995**, *47*, 135–141. [[CrossRef](#)]
58. Maruhashi, T.; Higashi, Y. Pathophysiological Association between Diabetes Mellitus and Endothelial Dysfunction. *Antioxidants* **2021**, *10*. [[CrossRef](#)]
59. Zhao, Q.; Zhu, L.; Wang, S.; Gao, Y.; Jin, F. Molecular Mechanism of the Anti-Inflammatory Effects of Plant Essential Oils: A Systematic Review. *J. Ethnopharmacol.* **2023**, *301*, 115829. [[CrossRef](#)]
60. Di Tomo, P.; Alessio, N.; Falone, S.; Pietrangelo, L.; Lanuti, P.; Cordone, V.; Santini, S.J.; Di Pietrantonio, N.; Marchisio, M.; Protasi, F.; et al. Endothelial Cells from Umbilical Cord of Women Affected by Gestational Diabetes: A Suitable In Vitro Model to Study Mechanisms of Early Vascular Senescence in Diabetes. *FASEB J.* **2021**, *35*, e21662. [[CrossRef](#)]
61. Di Pietro, N.; Formoso, G.; Pandolfi, A. Physiology and Pathophysiology of OxLDL Uptake by Vascular Wall Cells in Atherosclerosis. *Vasc. Pharm.* **2016**, *84*, 1–7. [[CrossRef](#)]
62. Pandolfi, A.; di Pietro, N.; Sirolli, V.; Giardinelli, A.; di Silvestre, S.; Amoroso, L.; di Tomo, P.; Capani, F.; Consoli, A.; Bonomini, M. Mechanisms of Uremic Erythrocyte-Induced Adhesion of Human Monocytes to Cultured Endothelial Cells. *J. Cell. Physiol.* **2007**, *213*, 699–709. [[CrossRef](#)]
63. Madonna, R.; Pandolfi, A.; Massaro, M.; Consoli, A.; de Caterina, R. Insulin Enhances Vascular Cell Adhesion Molecule-1 Expression in Human Cultured Endothelial Cells through a pro-Atherogenic Pathway Mediated by P38 Mitogen-Activated Protein-Kinase. *Diabetologia* **2004**, *47*, 532–536. [[CrossRef](#)]



64. Yuan, D.; Wang, Q.; Wu, D.; Yu, M.; Zhang, S.; Li, L.; Tao, L.; Harris, A.L. Monocyte-Endothelial Adhesion Is Modulated by Cx43-Stimulated ATP Release from Monocytes. *Biochem. Biophys. Res. Commun.* **2012**, *420*, 536–541. [[CrossRef](#)]
65. Di Tomo, P.; Di Silvestre, S.; Cordone, V.G.P.; Giardinelli, A.; Faricelli, B.; Pipino, C.; Lanuti, P.; Peng, T.; Formoso, G.; Yang, D.; et al. Centella Asiatica and Lipoic Acid, or a Combination Thereof, Inhibit Monocyte Adhesion to Endothelial Cells from Umbilical Cords of Gestational Diabetic Women. *Nutr. Metab. Cardiovasc. Dis.* **2015**, *25*, 659–666. [[CrossRef](#)]
66. Li, D.; Zhang, T.; Lu, J.; Peng, C.; Lin, L. Natural Constituents from Food Sources as Therapeutic Agents for Obesity and Metabolic Diseases Targeting Adipose Tissue Inflammation. *Crit. Rev. Food Sci. Nutr.* **2021**, *61*, 1947–1965. [[CrossRef](#)]
67. WHO: Good Harvest Processing Practices. 2017. Available online: [www.who.int/](http://www.who.int/) ... /V-2ndGlobalReview-RevisedDraft-WHO-GHPP-March2017.pdf (accessed on 16 June 2019).
68. WHO: Good Manufacturing Practices for Herbals. 2007. Available online: <http://apps.who.int/medicinedocs/s14215e/s14215e.pdf> (accessed on 18 May 2019).
69. Guo, R.W.; Yang, L.X.; Li, M.Q.; Liu, B.; Wang, X.M. Angiotensin II Induces NF-Kappa B Activation in HUVEC via the P38MAPK Pathway. *Peptides* **2006**, *27*, 3269–3275. [[CrossRef](#)]
70. Hajra, L.; Evans, A.I.; Chen, M.; Hyduk, S.J.; Collins, T.; Cybulsky, M.I. The NF-Kappa B Signal Transduction Pathway in Aortic Endothelial Cells Is Primed for Activation in Regions Predisposed to Atherosclerotic Lesion Formation. *Proc. Natl. Acad. Sci. USA* **2000**, *97*, 9052–9057. [[CrossRef](#)]
71. Paneni, F.; Costantino, S.; Battista, R.; Castello, L.; Capretti, G.; Chiodotto, S.; Scavone, G.; Villano, A.; Pitocco, D.; Lanza, G.; et al. Adverse Epigenetic Signatures by Histone Methyltransferase Set7 Contribute to Vascular Dysfunction in Patients With Type 2 Diabetes Mellitus. *Circ. Cardiovasc. Genet.* **2015**, *8*, 150–158. [[CrossRef](#)]
72. Zhu, J.; Wang, C.G.; Xu, Y.G. Lycopene Attenuates Endothelial Dysfunction in Streptozotocin-Induced Diabetic Rats by Reducing Oxidative Stress. *Pharm. Biol.* **2011**, *49*, 1144–1149. [[CrossRef](#)]
73. Di Pietro, N.; Baldassarre, M.P.A.; Cichelli, A.; Pandolfi, A.; Formoso, G.; Pipino, C. Role of Polyphenols and Carotenoids in Endothelial Dysfunction: An Overview from Classic to Innovative Biomarkers. *Oxid. Med. Cell. Longev.* **2020**, *2020*, 1–19. [[CrossRef](#)] [[PubMed](#)]
74. Timmers, S.; Konings, E.; Bilet, L.; Houtkooper, R.H.; Van De Weijer, T.; Goossens, G.H.; Hoeks, J.; Van Der Krieken, S.; Ryu, D.; Kersten, S.; et al. Calorie Restriction-like Effects of 30 Days of Resveratrol Supplementation on Energy Metabolism and Metabolic Profile in Obese Humans. *Cell Metab.* **2011**, *14*, 612–622. [[CrossRef](#)] [[PubMed](#)]
75. Castellano, I.; Di Tomo, P.; Di Pietro, N.; Mandatori, D.; Pipino, C.; Formoso, G.; Napolitano, A.; Palumbo, A.; Pandolfi, A. Anti-Inflammatory Activity of Marine Ovoidiol A in an In Vitro Model of Endothelial Dysfunction Induced by Hyperglycemia. *Oxid. Med. Cell. Longev.* **2018**, *2018*, 1–12. [[CrossRef](#)] [[PubMed](#)]
76. Baldassarre, M.P.A.; Di Tomo, P.; Centorame, G.; Pandolfi, A.; Di Pietro, N.; Consoli, A.; Formoso, G. Myoinositol Reduces Inflammation and Oxidative Stress in Human Endothelial Cells Exposed In Vivo to Chronic Hyperglycemia. *Nutrients* **2021**, *13*, 2210. [[CrossRef](#)]
77. Finicelli, M.; Di Salle, A.; Galderisi, U.; Peluso, G. The Mediterranean Diet: An Update of the Clinical Trials. *Nutrients* **2022**, *14*, 2956. [[CrossRef](#)]
78. Noad, R.L.; Rooney, C.; McCall, D.; Young, I.S.; McCance, D.; McKinley, M.C.; Woodside, J.V.; McKeown, P.P. Beneficial Effect of a Polyphenol-Rich Diet on Cardiovascular Risk: A Randomised Control Trial. *Heart* **2016**, *102*, 1371–1379. [[CrossRef](#)]
79. Ditano-Vázquez, P.; Torres-Peña, J.D.; Galeano-Valle, F.; Pérez-Caballero, A.I.; Demelo-Rodríguez, P.; Lopez-Miranda, J.; Katsiki, N.; Delgado-Lista, J.; Alvarez-Sala-Walther, L.A. The Fluid Aspect of the Mediterranean Diet in the Prevention and Management of Cardiovascular Disease and Diabetes: The Role of Polyphenol Content in Moderate Consumption of Wine and Olive Oil. *Nutrients* **2019**, *11*, 2833. [[CrossRef](#)]
80. Schwingshackl, L.; Christoph, M.; Hoffmann, G. Effects of Olive Oil on Markers of Inflammation and Endothelial Function—A Systematic Review and Meta-Analysis. *Nutrients* **2015**, *7*, 7651–7675. [[CrossRef](#)]
81. Garzoli, S.; Božović, M.; Baldisserotto, A.; Sabatino, M.; Cesa, S.; Pepi, F.; Vicentini, C.B.; Manfredini, S.; Ragno, R. Essential Oil Extraction, Chemical Analysis and Anti-Candida Activity of *Foeniculum Vulgare* Miller—New Approaches. *Nat. Prod. Res.* **2018**, *32*, 1254–1259. [[CrossRef](#)]
82. William, E. Wallace “Mass Spectra” by NIST Mass Spectrometry Data Center, in *NIST Chemistry WebBook, NIST Standard Reference Database Number 69*; Linstrom, P.J., Mallard, W.G., Eds.; National Institute of Standards and Technology: Gaithersburg, MD, USA, 2022; p. 20899.
83. Di Tomo, P.; Lanuti, P.; Di Pietro, N.; Baldassarre, M.P.A.; Marchisio, M.; Pandolfi, A.; Consoli, A.; Formoso, G. Liraglutide Mitigates TNF- $\alpha$  Induced pro-Atherogenic Changes and Microvesicle Release in HUVEC from Diabetic Women. *Diabetes Metab. Res. Rev.* **2017**, *33*, e2925. [[CrossRef](#)]

**Disclaimer/Publisher’s Note:** The statements, opinions and data contained in all publications are solely those of the individual author(s) and contributor(s) and not of MDPI and/or the editor(s). MDPI and/or the editor(s) disclaim responsibility for any injury to people or property resulting from any ideas, methods, instructions or products referred to in the content.